Phase-sensitive dc magnetometer based on magnetic–electromagnetic–magnetostrictive–piezoelectric heterostructure

Mingji Zhang, and Siu Wing Or

View Online   **Export Citation**   **CrossMark**

ARTICLES YOU MAY BE INTERESTED IN

Multiferroic magnetoelectric composites: Historical perspective, status, and future directions
Journal of Applied Physics **103**, 031101 (2008); https://doi.org/10.1063/1.2836410

A magnetoelectric sensor of threshold DC magnetic fields
Journal of Applied Physics **121**, 154503 (2017); https://doi.org/10.1063/1.4981533

Ultra-sensitive NEMS magnetoelectric sensor for picotesla DC magnetic field detection
Applied Physics Letters **110**, 143510 (2017); https://doi.org/10.1063/1.4979694

Phase-sensitive dc magnetometer based on magnetic–electromagnetic–magnetostrictive–piezoelectric heterostructure

Mingji Zhang[1,2] and Siu Wing Or[1,2,a]

[1]*Department of Electrical Engineering, The Hong Kong Polytechnic University, Hung Hom, Kowloon, Hong Kong*
[2]*Hong Kong Branch of National Rail Transit Electrification and Automation Engineering Technology Research Center, Kowloon, Hong Kong*

A phase-sensitive dc magnetometer is developed by combining a pair of permanent magnets, an electromagnetic coil, and a magnetostrictive–piezoelectric laminate in one direction to form a four-phase magnetic–electromagnetic–magnetostrictive–piezoelectric heterostructure. The dc magnetic field sensing in the magnetometer is based on the detection of the phase difference between the off-resonance magnetoelectric voltage manipulated by the dc magnetic field to be measured and the resonance electric current referenced at zero dc magnetic field, both under a preset bias magnetic field. The theoretical and experimental results confirm a high and linear dc magnetic field sensitivity of –0.21 °/Oe over a positive and negative dc magnetic field range of ±150 Oe with a small nonlinearity of 1.7%. The magnetometer has the ability to determine dc magnetic field direction and its sensitivity is independent of zero-field resonance electric current amplitude. © *2017 Author(s). All article content, except where otherwise noted, is licensed under a Creative Commons Attribution (CC BY) license (http://creativecommons.org/licenses/by/4.0/).* [http://dx.doi.org/10.1063/1.4975133]

I. INTRODUCTION

Magnetometers based on an extrinsic magnetoelectric (ME) effect in magnetostrictive–piezoelectric (MS–PE) laminates have stimulated considerable scientific research interest and technological development opportunity in the past decade owing to their promising features of passive sensing, high sensitivity, low noise, and wide bandwidth in comparison with conventional Hall-effect and magnetoresistance magnetometers.[1,2] In fact, the magnetic field sensing in most ME magnetometers is built on an extrinsic ac ME effect in which the magneto-mechano-electric coupling between the constituent MS and PE phases of the laminates is achieved dynamically under an applied ac magnetic field,[3,4] and the resulting magnetometers are classified as ac ME magnetometers.[5–8] The principal limitation in these ac ME magnetometers is their inability to measure dc magnetic fields because the extrinsic ac ME effect as characterized by an ME voltage or charge response is generally weakened by the decay of PE charge with time in the PE phase below 100 Hz.[1–3]

Recently, a current-mode dc ME magnetometer was proposed based on an ac electric current-controlled, dc magnetic field-induced Lorentz force effect in a conductive–PE heterostructure with or without dc magnetic biasing.[5,6] An ac electric current-controlled dc magnetic field sensitivity of 3–170 μV/Oe/A was obtained for dc magnetic fields up to 2 kOe under an ac control current of ≤300 mA at <15 kHz. More recently, a voltage-mode dc ME magnetometer was suggested based on an ac electric voltage-driven, dc magnetic field-tuned resonance dc ME effect in a transformer-like PE–MS heterostructure.[7,8] An ac electric voltage-controlled dc magnetic field sensitivity of

---

[a]Author to whom correspondence should be addressed: eeswor@polyu.edu.hk

–0.6 to –1.3 mV/Oe/V was acquired in a dc magnetic field range of 0–400 Oe at an ac driving voltage of ≤5 V at ~120 kHz. So far, the reported dc ME magnetometers fully rely on the detection of the amplitude of their ac electric voltage output to quantify the strength of the dc magnetic field input, and their sensitivities have the direct dependence on the amplitude of the ac control current or driving voltage. These amplitude-dependent detection techniques are liable to small-signal-induced inaccuracy and large-signal-induced nonlinearity and power consumption. By utilizing an output–input phase differencing technique, it would be possible to develop a phase-sensitive dc ME magnetometer with an amplitude-independent sensitivity and a high linearity.

In this paper, we report theoretically and experimentally a phase-sensitive dc ME magnetometer having a MS–PE laminate wound with an electromagnetic (EM) coil and sandwiched between a pair of permanent magnets in one direction to give a four-phase magnetic–EM–MS–PE heterostructure. Instead of detecting the ac electric voltage amplitude with respect to the dc magnetic field strength, our magnetometer detects the phase difference between the dc magnetic field-manipulated off-resonance ME voltage output from the MS–PE laminate of the heterostructure and the zero-field resonance electric current input to the EM coil of the heterostructure, both under a bias magnetic field preset by the permanent magnets to the heterostructure. As a result, our magnetometer exhibits a high and linear dc magnetic field sensitivity of –0.21 °/Oe, a two-sided measurement range of ±150 Oe, and a small nonlinearity of <2% under a small zero-field resonance electric current of 0.5 mA at 115.8 kHz and a low bias magnetic field of 150 Oe.

II. STRUCTURE AND WORKING PRINCIPLE

Figure 1(a) shows the schematic diagram and prototype of the proposed phase-sensitive dc magnetometer in the form of a four-phase magnetic–EM–MS–PE heterostructure. The heterostructure was fabricated by winding an EM coil on a MS–PE laminate, and the coil-wound MS–PE laminate was bonded by a pair of permanent magnets at its two ends. The MS–PE laminate was prepared by bonding a Pb(Zr, Ti)O$_3$ (PZT, CeramTec P8) PE ceramic plate of 12 mm length (l), 6 mm width (w), and 1 mm thickness (t) between two [112]-textured Tb$_{0.3}$Dy$_{0.7}$Fe$_{1.92}$ (Terfenol-D, Baotou Rare Earth) MS alloy plates of the same dimensions in the thickness direction. The polarization (P) direction of the PE ceramic plate and the magnetization (M) direction of the MS alloy plates were oriented along their thickness and length directions, respectively. The EM coil was formed by winding two layers of AWG#26 enameled copper wire in the clockwise direction to give a total of 64 turns (n), with
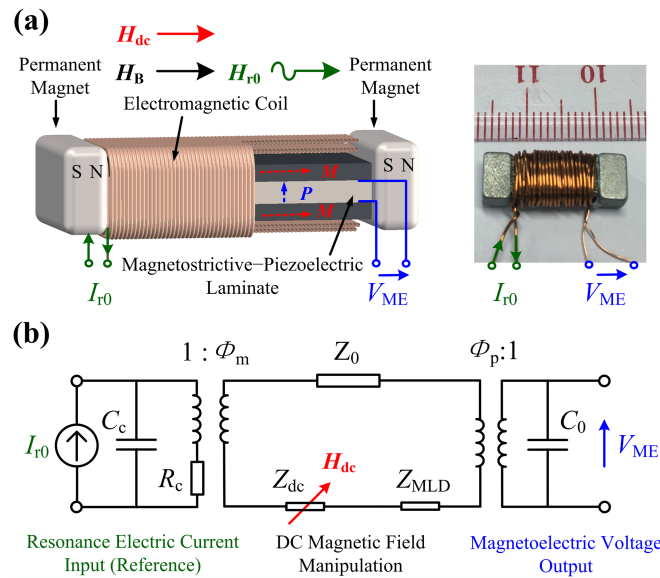

FIG. 1. (a) Schematic diagram and prototype of the proposed phase-sensitive dc magnetometer. (b) Dynamic magneto-mechano-electric equivalent circuit of the magnetometer.

each layer comprising 32 turns. The two permanent magnets were length-magnetized NdFeB slabs having 4 mm length, 8 mm width, and 4 mm height. These permanent magnets were able to preset an average bias magnetic field of 150 Oe along the length of the MS–PE laminate for enabling a two-sided measurement of dc magnetic fields up to ±150 Oe and an ability to determine the direction of dc magnetic fields.

The working principle of the phase-sensitive dc magnetometer in Fig. 1(a) can be described by the biasing of the heterostructure with a bias magnetic field (H_B = 150 Oe) preset by the permanent magnets, and on the basis of this H_B and the natural resonance frequency of the heterostructure without the dc magnetic field to be measured ($f_{r0} \equiv f_r$ at H_{dc} = 0 Oe under H_B), the detection of the phase difference ($\theta = \theta_{V_{ME}} - \theta_{I_{r0}}$) between the off-resonance ME voltage (V_{ME}) output from the MS–PE laminate of the heterostructure under the manipulation of H_{dc} to be measured and the resonance electric current (I_{r0}) input to the EM coil of the heterostructure at zero H_{dc}. In more details, the heterostructure is preset to have built-in magnetic biasing by H_B (=150 Oe) to produce a MS strain (λ_0) and hence an elastic modulus (E_0) and f_{r0} in the absence of both I_{r0} and H_{dc}. By inputting a small-signal I_{r0} into the EM coil, a small-signal resonance magnetic field (H_{r0}) is generated along the length of the heterostructure and to vary about H_B at f_{r0} in accordance with Ampère's law. The heterostructure is excited by this H_{r0} to resonate at its f_{r0}, thereby producing a resonance ME voltage (V_{MEr0}) with its phase angle ($\theta_{V_{MEr0}}$) leading that of $I_{r0}(\theta_{I_{r0}})$ by 90° (i.e., $\theta_0 = \theta_{V_{MEr0}} - \theta_{I_{r0}} = 90°$) in light of the resonance ME effect in the MS–PE laminate. In the presence of a positive/negative H_{dc}, the initially preset λ_0 and hence E_0 and f_{r0} are manipulated by H_{dc} with respect to H_B (i.e., $H_B \pm H_{dc}$), giving a larger/smaller λ and hence a smaller/larger E and a lower/higher f_r based on the negative $-\Delta E$ effect intrinsic in all MS materials and devices.[5,6] This, in turn, alters V_{MEr0} to become V_{ME} with respect to I_{r0}, leading to a larger/smaller amplitude ($|V_{ME}|$) as well as smaller/larger $\theta_{V_{ME}}$ and θ.

Figure 1(b) illustrates the dynamic magneto-mechano-electric equivalent circuit of the magnetometer in Fig. 1(a). The equivalent circuit consists of three sections, namely the resonance electric current input (reference) section, the dc magnetic field manipulation section, and the ME voltage output section. In the resonance electric current input section, the generation of H_{r0} at f_{r0} by I_{r0} in the EM coil and the coupling of the generated H_{r0} to the MS–PE laminate in the dc magnetic field manipulation section are modeled by a I_{r0}-dependent magneto-mechanical transformer (Φ_m) and a coil resistor (R_C) connected in parallel with a coil parasitic capacitor (C_C).[9] In the dc magnetic field manipulation section, the excitation of the MS–PE laminate by the coupled H_{r0} at f_{r0} under H_B preset by the permanent magnets and the manipulation of H_{dc} with respect to H_B are modeled as a characteristic acoustic impedance of the MS–PE laminate in the presence of H_B (Z_0) in series with two characteristic acoustic impedances caused by the manipulation effect of H_{dc} (Z_{dc}) and the mass loading and damping effects of the EM coil and the permanent magnets (Z_{MLD}) so that the effective characteristic acoustic impedance (Z_{eff}) is the sum of Z_0, Z_{dc}, and Z_{MLD}.[10] In the ME voltage output section, the output of V_{ME} due to the off-resonance ME effects with the H_{dc} manipulation is modeled by a mechanoelectric transformer (Φ_p) in parallel with a clamped capacitance (C_0).[11] Since the phase shift caused by R_c and C_c is a constant and can be compensated by a zeroing compensation means in practice (see Eq. (6) and Sec. III for further explanation), R_c and C_c can be neglected from the equivalent circuit. Physically, Z_{eff}, Φ_m, Φ_p, and C_0 can be expressed as follows:

$$Z_{eff} = Z_0 + Z_{dc} + Z_{MDL}; Z_0 = -\frac{1}{2}j\sqrt{\frac{\rho}{s_0}}\tan^{-1}\left(\pi f l \sqrt{\rho s_0}\right) \tag{1}$$

$$\Phi_m = 2wt\frac{d_{33,m0}}{s_0}H_{r0}; H_{r0} = \frac{nI_{r0}}{l} \tag{2}$$

$$\Phi_p = \frac{wd_{31,p}}{s_0} \tag{3}$$

$$C_0 = \frac{wl}{t}\varepsilon_{33}^T(1 - k_{31}^2) \tag{4}$$

where $\rho = (2\rho_m + \rho_p)/3$ and $s_0 = 3s_{11}^E s_{330}^H/(s_{11}^E + 2s_{330}^H)$ are the density and H_B-preset compliance of the MS–PE laminate, respectively; $d_{33,m0}$ and s_{330}^H are the H_B-preset piezomagnetic and compliance

coefficients of the MS phase, respectively; ε_{33}^T, $d_{31,\text{p}}$, and k_{31} are the permittivity, piezoelectric, and electromechanical coupling coefficients of the PE phase, respectively.[12,13] By solving the equivalent circuit in Fig. 1(b), the H_{dc}-manipulated resonance frequency (f_r) of the heterostructure can be expressed as

$$f_\text{r} = \frac{1}{2l}\sqrt{\xi\rho\left(\frac{3s_{11}^E s_{33}^H}{s_{11}^E + 2s_{33}^H}\right)} \tag{5}$$

where ξ is a constant (=1.77 in our case) for accounting the contribution of Z_{MLD} and s_{33}^H is the H_{dc}-manipulated compliance coefficient of the MS phase. The H_{dc}-manipulated phase difference (θ) between $\theta_{V_{\text{ME}}}$ and $\theta_{I_{\text{r0}}}$ can be expressed as

$$\theta = \arctan\frac{(f_{\text{r0}}/f_\text{r})}{1 - (f_{\text{r0}}/f_\text{r})^2} + \varphi_0 \tag{6}$$

where φ_0 is introduced to include the phase shift caused by R_c, C_c as well as any other nonlinearity and uncertainty in practice. The value of φ_0 can be compensated by a zeroing compensation means to be described in Sec. III. It is noted that θ is a nonlinear and implicit function of H_{dc} in Eq. (6). The tremendous slope of arctan function when f_{r0}/f_r is close to unity gives an approximately linear response of θ with respect to H_{dc}. Therefore, the dc magnetic field sensitivity (S_θ) of the magnetometer can be quantified by the slope of the θ versus H_{dc} plot as

$$S_\theta = \text{d}\theta/\text{d}H_{\text{dc}}. \tag{7}$$

It is interesting to note that θ in Eqs. (6) and (7) is independent of I_{r0}. This independence can effectively minimize the small ac current and voltage amplitude-induced inaccuracy as well as the large ac current and voltage amplitude-induced nonlinearity and power consumption intrinsic in the previously reported current- and voltage-mode dc ME magnetometers, respectively.[5–8]

III. EXPERIMENTS

Figure 2 illustrates the schematic diagram of the experimental setup for the evaluation of the phase-sensitive dc magnetometer at room temperature (~20 °C). The evaluation involves: 1) applying a swept sinusoidal electric current (I) of controlled amplitude (i.e., 0.5 and 1 mA peak) to the EM coil of the heterostructure in the vicinity of resonance of 113–119 kHz, and 2) measuring the corresponding V_{ME} output from the MS–PE laminate of the heterostructure at discrete frequency (f) intervals of 100 Hz/step under the manipulation of various H_{dc} from –150 to 150 Oe along the length of the heterostructure, to give the f dependence of both amplitude ($|V_{\text{ME}}|$) and phase angle ($\theta_{V_{\text{ME}}}$) of V_{ME} at various H_{dc} and I. The swept sinusoidal I was provided by a constant-current supply amplifier (Techron 7572) connected to an arbitrary waveform generator (Agilent 33210A) and was monitored by a current probe and its amplifier (HIOKI 3271). The monitored I was fed into a lock-in amplifier (SRS SR865) with a phase compensation for φ_0 in Eq. (6), if any. The H_{dc} manipulation was generated using a pair of Helmholtz coils under the control of a dc current supply (RIGOL
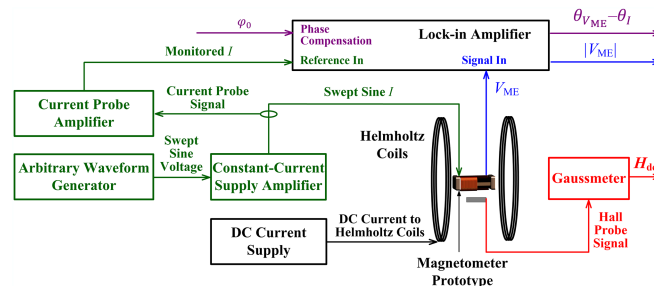

FIG. 2. Schematic diagram of the experimental setup.

DP811A) and was monitored using an axial Hall probe connected to a Guassmeter (F.W. Bell 7030). The H_{dc}-manipulated V_{ME} with respect to I was measured using the lock-in amplifier to give $|V_{ME}|$ and $\theta_{V_{ME}} - \theta_I$ as the outputs.

IV. RESULTS AND DISCUSSION

Figure 3(a) shows the measured f dependence of $|V_{ME}|$ in the vicinity of resonance of 113–119 kHz at various H_{dc} from −150 to 150 Oe under two different I of 0.5 and 1 mA peak. For I = 1 mA and H_{dc}=0 Oe (i.e., the curve with large black solid square), the heterostructure is found to resonate at f_{r0}=115.8 kHz with $|V_{MEr0}|$=1.2 mV. An increase/a decrease in H_{dc} from 0 Oe shifts the resonance curves in such ways that their $|V_{MEr}|$ appear on the higher/lower $|V_{ME}|$ side while their f_r occur on the lower/higher f side. This is a valid evidence of the H_{dc}-manipulated resonance ME effect in the heterostructure described in Secs. I and II. In other words, an increase in H_{dc} from 0 to 150 Oe will manipulate the initially H_B-preset λ_0 and hence E_0, f_{r0}, and V_{MEr0} to become a larger λ and hence a smaller E, a lower f_r, and a higher $|V_{MEr}|$ in accordance with the decreasing trend in the negative−ΔE effect.[5,6] The situation is reversed upon the reversal of H_{dc} from 0 to −150 Oe. Now, if I is set as I_{r0} with f_{r0} = 115.8 kHz, an increase/a decrease in H_{dc} from 0 Oe will increase/decrease the value of $|V_{MEr0}|$ to become $|V_{ME}|$ (along the dash line) as a result of the shift in resonance curves. This suggests the existence of a direct relationship between $|V_{ME}|$ and H_{dc} on I_{r0}. When I is reduced to 0.5 mA, all the $|V_{ME}|$ spectra exhibit very similar quantitative trends to those at I = 1 mA, except that their $|V_{ME}|$ values are half-reduced at the same H_{dc}. The observation indicates the dependence of the amplitude of I_{r0} on the sensitivity of our magnetometer if $|V_{ME}|$ is used to quantify H_{dc}. Having been described in Sec. I, the use of the amplitude-dependent detection technique, as in the reported current- and voltage-mode dc ME magnetometers,[5–8] will lead to the deficiencies of amplitude-dependent sensitivity, small-signal-induced inaccuracy, and large-signal-induced nonlinearity and power consumption. By contrast, the shift in f_r with H_{dc} provides an essential indication for realizing amplitude-independent sensitivity, high linearity, and low power consumption in our magnetometer by utilizing an output–input phase differencing technique through the detection of θ ($= \theta_{V_{ME}} - \theta_{I_{r0}}$), instead of $|V_{ME}|$.

Figure 3(b) shows the measured and calculated f dependence of $\theta_{V_{ME}} - \theta_I$ in the vicinity of resonance of 113–119 kHz at various H_{dc} from −150 to 150 Oe under two different I of 0.5 and 1 mA peak. The calculation was performed by substituting f_{r0} = 115.8 kHz obtained in Fig. 3(a) and supplier-provided material parameters (i.e., ρ_m = 9200 kg/m³, ρ_p = 7600 kg/m³, s_{33}^H = 32.1 + 6.4 × 10⁻⁴ · H_{dc} pm²/N, and s_{11}^E = 7.28 pm²/N) into Eqs. (5) and (6). The measured and calculated $\theta_{V_{ME}} - \theta_I$ spectra
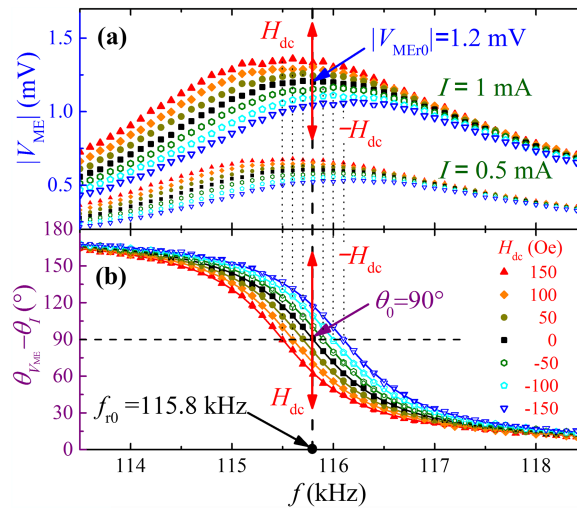

FIG. 3. (a) Measured f dependence of $|V_{ME}|$ and (b) measured (symbols) and calculated (lines) f dependence of $\theta_{V_{ME}} - \theta_I$ in the vicinity of resonance of 113–119 kHz at various H_{dc} from −150 to 150 Oe under two different I of 0.5 and 1 mA peak.
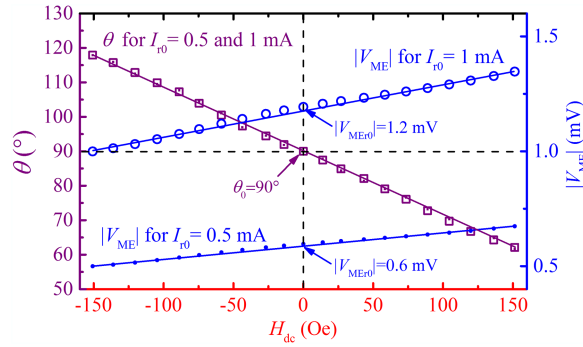
FIG. 4. Measured (symbols) $|V_{ME}|$ and θ in the H_{dc} range of ±150 Oe for two different I_{r0} of 0.5 and 1 mA peak, both at $f_{r0} = 115.8$ kHz. The lines are the fitted lines to the measured data.

under two different I overlap fully with each other, elucidating a practically viable measurement of H_{dc} by detecting I-independent $\theta_{V_{ME}} - \theta_I$. For a given I, the measured and calculated spectra also agree well with each other, confirming the validity of our physical model in Sec. II. In fact, the $\theta_{V_{ME}} - \theta_I$ spectra essentially follow the arctan trends for all H_{dc} in that their slopes give an approximately linear response of θ with respect to H_{dc} when f_{r0}/f_r is close to unity. Considering the case of $H_{dc} = 0$ Oe (i.e., the curve with black solid square), the heterostructure resonates at $f_{r0} = 115.8$ kHz with $\theta_{V_{MEr0}} - \theta_{I_{r0}} = \theta_0 = 90°$. Applying a positive/negative H_{dc} will shift f_r to the lower/higher f side (Fig. 3(a)), giving rise to the corresponding shift in $\theta_{V_{MEr}} - \theta_{I_r} = 90°$ to the lower/higher f side. Now, if I is kept as I_{r0} with $f_{r0} = 115.8$ kHz, an increase/a decrease in H_{dc} from 0 Oe will decrease/increase the value of $\theta_0 = \theta_{V_{MEr0}} - \theta_{I_{r0}} = 90°$ to become $\theta = \theta_{V_{ME}} - \theta_{I_{r0}}$ (along the dash line). This reflects the presence of a direct relationship between θ and H_{dc} on I_{r0}.

Figure 4 plots the measured $|V_{ME}|$ and θ in the H_{dc} range of ±150 Oe for two different I_{r0} of 0.5 and 1 mA peak, both at $f_{r0} = 115.8$ kHz. The values of $|V_{ME}|$ and θ are extracted from their corresponding spectra at $f_{r0} = 115.8$ kHz (Fig. 3). It is clear that $|V_{ME}|$ for $I_{r0} = 0.5$ and 1 mA exhibit two separate, linear increasing/decreasing trends from 0.6 and 1.2 mV (i.e., $|V_{MEr0}|$), respectively, when H_{dc} is increased/decreased from 0 Oe. In contrast, θ for $I_{r0} = 0.5$ and 1 mA demonstrate almost identical and linear decreasing/increasing trends from 90° (i.e., θ_0) when H_{dc} is increased/decreased from 0 Oe. By linear-fitting the plots of $|V_{ME}|$ versus H_{dc} and those of θ versus H_{dc} to obtain the slopes, the dc magnetic field sensitivity for θ (S_θ) is found to be –0.21 °/Oe for both $I_{r0} = 0.5$ and 1 mA with a small nonlinearity of 1.7% in the H_{dc} range of ±150 Oe, while that for $|V_{ME}|$ ($S_{|V_{ME}|}$) is determined to be 0.53 and 1.06 μV/Oe with nonlinearities of 3.5 and 2.3% for $I_{r0} = 0.5$ and 1 mA, respectively, in the same H_{dc} range. It is important to note that S_θ is independent of the amplitude of I_{r0}, but it is not the case for $S_{|V_{ME}|}$. The I_{r0}-dependent $S_{|V_{ME}|}$ is expressed as 1.06 μV/Oe/mA.

V. CONCLUSION

We have developed a phase-sensitive dc ME magnetometer based on a four-phase magnetic–EM–MS–PE heterostructure and evaluated theoretically and experimentally its working principle and characteristics. The results have confirmed a unique detection of the phase difference ($\theta = \theta_{V_{ME}} - \theta_{I_{r0}}$) between V_{ME} output and I_{r0} input, both under the manipulation of H_{dc} to be measured and a H_B preset in the heterostructure. The magnetometer has demonstrated a high and linear S_θ of –0.21 °/Oe, a two-sided H_{dc} measurement range of ±150 Oe, and a small nonlinearity of 1.7% under a small I_{r0} of 0.5 mA at f_{r0} of 115.8 kHz and a low H_B of 150 Oe. By contrast, the amplitude-dependent detection has resulted in two different $S_{|V_{ME}|}$ of 0.53 and 1.06 μV/Oe with increased nonlinearities of 3.5 and 2.3% for $I_{r0} = 0.5$ and 1 mA, respectively, giving a I_{r0}-dependent $S_{|V_{ME}|}$ of 1.06 μV/Oe/mA, in the same H_{dc} range. This phase-sensitive dc ME magnetometer is capable of broadening the scientific and technological scopes of ME magnetometers in general, and dc ME magnetometers in specific.

[1] C. W. Nan, M. I. Bichurin, S. X. Dong, D. Viehland, and G. Srinivasan, J. Appl. Phys. **103**, 031101 (2008).
[2] R. S. Popovic, J. A. Flanagan, and P. A. Besse, Sens. Actuators A Phys. **56**, 39 (1996).
[3] P. P. Freitas, R. Ferreira, S. Cardoso, and F. J. Cardoso, Phys. Condens. Mat. **19**, 165221 (2007).
[4] J. Zhai, S. Dong, Z. Xing, J. Li, and D. Viehland, Appl. Phys. Lett. **91**, 123513 (2007).
[5] C. M. Leung, S. W. Or, and S. L. Ho, J. Appl. Phys. **107**, 09E702 (2010).
[6] L. Zhang, S. W. Or, C. M. Leung, and S. L. Ho, J. Appl. Phys. **114**, 027016 (2013).
[7] L. Zhang, S. W. Or, C. M. Leung, and S. L. Ho, J. Appl. Phys. **115**, 17E520 (2014).
[8] L. Zhang, S. W. Or, and C. M. Leung, J. Appl. Phys. **117**, 17A748 (2015).
[9] X. Dong, Y. Wu, J. Wan, T. Wei, Z. Zhang, S. Chen, H. Yu, and J. Liu, J. Phys. D: Appl. Phys. **41**, 035003 (2008).
[10] A. Lohfink and P.-C. Eccardt, IEEE Trans. Ultrason. Ferroelectr. Freq. Control **52**, 2163 (2005).
[11] S. Dong, J.-F. Li, and D. Viehland, IEEE Trans. Ultrason., Ferroelect., Freq. Control **50**, 1253 (2003).
[12] D. Damjanovic, Rep. Prog. Phys. **61**, 1267 (1998).
[13] J. Zhai, Z. Xing, S. Dong, J. Li, and D. Viehland, J. Am. Ceram. Soc. **91**, 351 (2008).